Advances in Biological Liquid Crystals

Dr. Jianguo Zhao[1], Dr. Utku Gulan[2], Dr. Takafumi Horie[3], Prof. Naoto Ohmura[3],

Dr. Jun Han[4], Prof. Chao Yang[5], Prof. Jie Kong[6], Dr. Steven Wang[7*], Dr. Ben Bin Xu[8*]*

[1]Dr. J. G. Zhao
Quanzhou Institute of Equipment Manufacturing, Haixi Institutes,
Chinese Academy of Sciences, Quanzhou, 362200, China

Third Institute of Physics—Biophysics,
University of Göttingen, Göttingen, 37077, Germany

[2]Dr. U. Gulan
Institute of Environmental Engineering,
ETH Zurich, Zurich, 8093, Switzerland

[3]Dr. T. Horie, Prof. N. Ohmura
Department of Chemical Science and Engineering,
Kobe University, Kobe, 657-8501, Japan

[4]Dr. J. Han
Quanzhou Institute of Equipment Manufacturing ,
Haixi Instutes,
Chinese Academy of Sciences, Quanzhou, 362200, China

[5]Prof. C. Yang
CAS Key Laboratory of Green Process and Engineering,
Institute of Process Engineering,
Chinese Academy of Sciences, Beijing, 100190, China

[6]Prof. J. Kong
Shaanxi Key Laboratory of Macromolecular Science and Technology, School of Science, Northwestern Polytechnical University, Xi'an, 710072, P. R. China
*Corresponding Author, E-mail: kongjie@nwpu.edu.cn

[7]Dr. S. Wang
School of Engineering,
Newcastle University,
Newcastle Upon Tyne, NE1 7RU, UK
*Corresponding Author, E-mail: steven.wang@newcastle.ac.uk

[8]Dr. B. B. Xu
Mechanical and Construction Engineering, Faculty of Engineering and Environment,
Northumbria University,
Newcastle upon Tyne, NE1 8ST, UK
*Corresponding Author, E-mail: ben.xu@northumbria.ac.uk

Keywords: biological soft matter, phase transition, active liquid crystal

Abstract:

Biological Liquid Crystal, a rich set of soft materials with rod-like structures widely existed in nature, possess typical lyotropic liquid crystalline phase properties both in vitro (e.g. cellulose, peptides and protein assemblies), and in vivo (e.g. cellular lipid membrane, packed DNA in bacteria and aligned fibroblasts). Given the ability to undergo phase transition in response to various stimuli, numerous practices have been exercised to spatially arrange biological liquid crystals. In this mini-review, the fundamental understanding of interactions between rod-shaped biological building blocks and their orientational ordering across multiple length scales is addressed. Discussions are made with regard to the dependence of physical properties of non-motile objects on the first-order phase transition and the coexistence of multi-phases in passive liquid crystalline systems. This review also focuses on how the applied physical stimuli drives the reorganization of constituent passive particles for a new steady-state alignment. A number of recent progresses in the dynamics behaviours of active liquid crystals are presented, and particular attention has been given to those self-propelled animate elements, like the formation of motile topological defects, active turbulence, correlation of orientational ordering and cellular functions. Finally, future implications and potential applications of the biological liquid crystalline materials are discussed.

1. Introduction

The liquid crystalline (LC) phase is an intermediate state that could flow like amorphous liquid and is partially orient like solid crystal. Conventional passive liquid crystals are composed of non-motile building blocks. To reach the LC state, the constituent molecules or molecular assemblies should be geometrically anisotropic in shape, such as disc, bowl and rod-like configurations. At the equilibrium state, the phase transition may occur by varying thermal conditions (thermotropic LC) or component concentration in solvent (lyotropic LC).

A variety of inanimate, passively diffusing rod-shaped biological materials are capable to form lyotropic LC, [1-4] where the entropic interaction plays an essential role in stabilising LC in a specific order. Onsager draw a theoretical understanding for this first-order isotropic-nematic phase transition based on hard-core interaction between particles: [5]

$$c = \emptyset L/D \qquad (1)$$

where c is the dimensionless concentration, $\emptyset$ the volume fraction of suspended rods, L the length and D the diameter. The phase transition originated from the competition between orientational entropy-rod tending to become orientationally disordered, and packing/free volume entropy, which is increased for aligned rods. At low volume fraction, the rods are randomly dispersed in a completely isotropic state. Once above the critical concentration $\emptyset_I$, the rods start to nucleate and grow into an ordered domain, termed as tactoid, yield a co-existence of isotropic and nematic layers in an equilibrium state. When the volume fraction of rods exceeds the $\emptyset_N$, the phase transits into a full nematic state having a high order parameter, where all rods preferably orientate their long axis along a common direction. The average orientation is termed as director n, and the scalar order parameter is represented by:

$$S = \langle \frac{3\cos^2\theta - 1}{2} \rangle \qquad (2)$$

where θ is the angle between the molecular long axis and director. $S = 0$ for an isotropic phase, whereas an absolutely ordered phase $S = 1$. The nematic phase is the most common LC phase, having long-range orientational ordering but no positional ordering of components. In case the rods are mono-dispersed, the smectic phase may form with increased volume fraction,

where the aligned rods form one-rod-length monolayer, and illustrated orientational and positional order. In the last decades, the correlation of microscopic interactions to macroscopic LC collective behaviours has been extensively explored via a combination of theoretical description and experimental observations. [6-9] Moreover, LC materials also show promising potentials in materials science and practical applications [10-14], due to the ordered organizations in multi-length scales and high susceptibility to various stimuli. [15-23]

Active biological LC that is composed of animate and self-propelled constituents, has attracted much attention recently. Striking collective behaviours and exciting properties have been identified, including the continuous transduction of internal energy into active stress and corresponding motion of individual biological filaments, the local alignment between neighbouring rods, and the large-range evolution of orientational ordered domains. The active LC behaviours are remarkably distinct from the conventional passive LC in various aspects. Instead of external fields from outside (e.g. magnetic or electric), the self-sustained active LC emerges from internal energy at the level of individual constituents. The rod-shaped building blocks continuously convert energy stored in adenosine triphosphate (ATP) into mechanical forces and motion. [24] The dynamically steady LC behaviours cannot be well understood by minimization of thermodynamic potential, because of the continuous energy conversion and consumption. In addition, only the nematic phase, rather than higher ordering state (e.g. smectic phase), has been monitored till now, mostly because of the robust motion driven by internal force and the polydispersity of sub-units. [25] On the other hand, the active LC system shares some common characteristics with the conventional passive LC. For example, the active LC phase shows association with constituent density. [26-30] Above critical particle density, they spontaneously organize into a wide variety of large-scale collective behaviours with remarkably complex behaviours, [31] including pattern formation, [29, 32] fluid flow, [33-35] and motile topological defects. [36, 37] In addition, the active LC must break symmetry in the ordered collective motion, meaning a preferable direction when bulk particles act together. Overall, this is a rapidly developing field that combines soft condensed matter physics,

molecular biology and biophysics, while multiple interesting structural, dynamic and mechanical features remain largely elusive.

2. The physical properties of the constituents in passive LC

The passive LC system, which consists of inanimate biological constituents dispersed in an aqueous environment, could generate intriguing complex behaviours by the steric interactions between particles. The examples range from DNA, [38-45] collagen, [46] neurofilaments, [47] and cellulose, [48-51] to non-motile virus complexes. [52-55] In addition, many protein assemblies exhibit fascinating LC phase behaviours, for example like beta-lactoglobulin, [56-61] lysozyme, [62, 63] and insulin. [64] In this section, we focus mainly on key aspects that are crucial to the fundamental question of how the physical properties of building blocks, including rod aspect ratio (length-to-diameter, L/D), polydispersity, flexibility and surface charge affect the macroscale isotropic-nematic phase transition and corresponding coexistence. It is worth mentioning that a comprehensive consideration of multi-factors is needed in the fundamental understandings of LC phase behaviours. Due to the complexity of the experimental system, the phase behaviours are sometimes much more complicated than theoretical predictions under simplified conditions.

2.1 Aspect ratio

Aspect ratio is the central parameter for the LC phase formation. First of all, the thermodynamically stable nematic phase requires a high anisotropy (approximately $L/D \geq 4$). [65, 66] Second, the isotropic-nematic transition concentration is correlated to the L/D of rods (equation 1), as evidenced by both theoretical predictions and experimental findings. [5, 56] Lastly, the concentration range of the isotropic-nematic coexistence is $\Delta\phi = (c_N\text{-}c_I)\, D/L$. Thus, one sees the biphasic phase only when the aspect ratio is at an appropriate range. [67]

2.2 Polydispersity

The modified Onsager theory predicted that polydispersity facilitates the phase separation. In the mixture of rod-shaped particles with different lengths, the system achieves

the onset of isotropic-nematic coexistence at a lower volume fraction than that of one component case. [68] Moreover, their polydispersity widens the isotropic-nematic coexistence region, and the long rods tend to accumulate in the nematic phase rather than the isotropic phase. [68, 69] The polydispersed rods may also enrich the multi-phase coexistence having distinct densities, including the nematic-nematic biphasic phase, and isotropic-nematic-nematic triphasic phases, as predicted by the Onsager treatment, [69-71] and lattice model. [72] Indeed, in the mixture *fd* virus with varied thickness, interesting 2 and 3-phase coexistence were experimentally observed at equilibrium state. [53]

2.3 Flexibility

One essential mechanical parameter to quantify the bending stiffness of biological filaments is so-called persistence length, defined as the length over which the thermal fluctuations start to bend the rods. [73] The competition between the entropic tendency of a crinkle as a random coil and bending energetic that prefers straight construction, leads to the dramatic mechanical properties of biopolymers, [74] significantly affecting their LC phase behaviours. [54, 75] As soon as rods exhibit very little flexibility, the system would compete against rotational and internal bending contributing to the total entropy. In general, flexibility drives the nematic phase to emerge at a higher concentration; the coexistent concentration range gets narrow and the corresponding order parameter is decreased, when compared to the stiff rods. [76-78] In the case of very flexible polymers, no LC domain could be observed even at critically high concentrations, due to the small persistence length.

2.4 Electrostatic interaction

Abundant biopolymers are polyelectrolytes, and the electrostatic repulsion between particles strongly affects the orientational organization. [52, 79, 80] The effective diameter (D_{eff}) includes the object diameter and electric double layer. D_{eff} is dependent on the balance between the surface charge and bulk ionic strength. Ions screen the electrostatic double layer repulsion of particles. Thus, D_{eff} decreases with an increase of ionic strength; the phase transition therefore occurs at a higher critical concentration. [81, 82]

3. Additional physical stimuli-induced LC behaviour

In general, the biological constituents in LC are tiny and remarkably sensitive to physical stimuli such as fluid flows, magnetic/electric fields, temperatures, and pH values. The additionally applied field could guide striking dynamics and induce collective reorientation in the nanoscale, which essentially gives rise to a new steady-state ordering on a large scale. [83]

3.1 Depletion interaction

The additional non-adsorbing polymer in colloidal suspension induces an attraction between rod-shaped particles, driving the LC phase transition to lower rod concentration. In the dilute polymer solution, the strength of depletion interaction is dominated by the polymer concentration and its range is dependent on polymer size. The addition of polymer widens the concentration range of the isotropic-nematic biphasic phase, where polymer prefers partitions into isotropic phase and the rods stay in the nematic phase. [84-86] This phenomenon could be explained by the Asakura-Oosawa model: polymer coils are treated as inter-penetrable spheres of radius R, but they feel colloidal particles via hard-core repulsion. When the surface-surface distance between two colloidal particles is smaller than R, the polymer would be excluded from the gap, giving rise to an imbalance in osmotic pressure responsible for the attractive depletion force between particles. [87, 88] In the semi-dilute polymer regime, the depletion strength and range are correlated to the polymer concentration. With an increase in polymer concentration, the depletion strength increases steadily; while the polymer mesh size becomes smaller, leading to a shorter depletion range. [89] The long-range electrostatic repulsive force screens the contribution of depletion attraction at high enough polymer concentration, at which a stable single phase exists. Indeed, Zhao et al. observed the expanding of the isotropic-nematic biphasic region, and then restabilization by gradually increasing the concentration of non-adsorbing polymer in amyloid fibrils suspension (**Figure 1**a-d). [58]

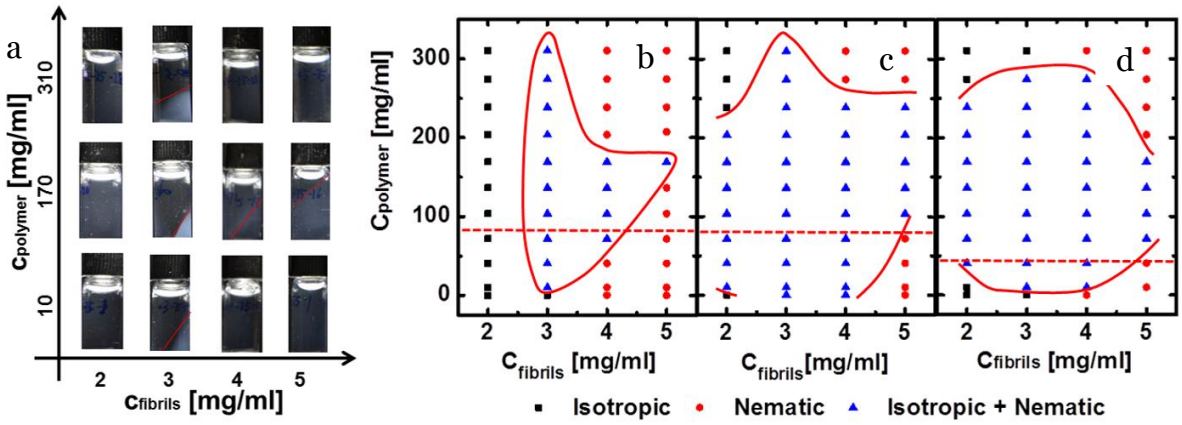

Figure 1. (a) The phase diagram of amyloid fibrils and non-adsorbing polymers mixture observed under normal light. (b) The isotropic-nematic biphasic region exits only at intermediate polymer concentration. The coexistence is inflated by increasing ionic strength (c) and the molecular weight of depleted polymer (d). [58]

3.2 Temperature

The structural flexibility of many biological materials correlates to temperature. [90-92] For example, Fraden reported that the flexibility of the *fd* virus changes in a non-monotonic fashion with a temperature range over 4-70 °C and amplifies into a shift of concentration range of macroscopic isotropic-nematic coexistence. [54] Moreover, the temperature dependence of cholesteric interaction has been recently explored in biological LC. [93, 94] For example, Dogic indicated that in the mixture of rod-like *fd* virus and dextran, the particles self-organize into membrane of one-rod-length-thick monolayer at high temperature, with rods parallel to neighboring particles in the interior, and twisted near the edge. With decreasing temperature, the rod's chirality significantly increases, resulting in larger twist angles that are applied to minimize the rod interaction energy. Thus, the 2D membrane becomes remarkably unstable due to the decrease of its edge tension, and undergoes a transition into 1D twisted ribbon (**Figure 2**a-d). [95-98] Recently, This interesting experimental structures phenome has been quantitatively explained via entropically-motivated theory (Figure 2e-g). [98] Another interesting temperature-dependent behaviour is the particle motion under temperature gradients that enables significant drift toward a

specific direction, thus generating spatial variations of concentration in the field director. [99] The peculiar properties of biopolymers, like net charge, amphiphilic surfaces and salt-specificity effects, make the particle-solvent interfacial interaction strongly dependent on temperature. [100, 101] By placing the amyloid fibrils suspension in a straight microfluidics channel, having a temperature gradient between the 2 parallel walls, Zhao et al. found that the thermophoretic force drove migration of the component toward the hot side when average T < 55°C, and an isotropic-nematic coexisting phase was achieved at saturation. When $T \geq 55$°C, the fibrils shift into a thermophilic property by moving to the cold side preferably. [61]

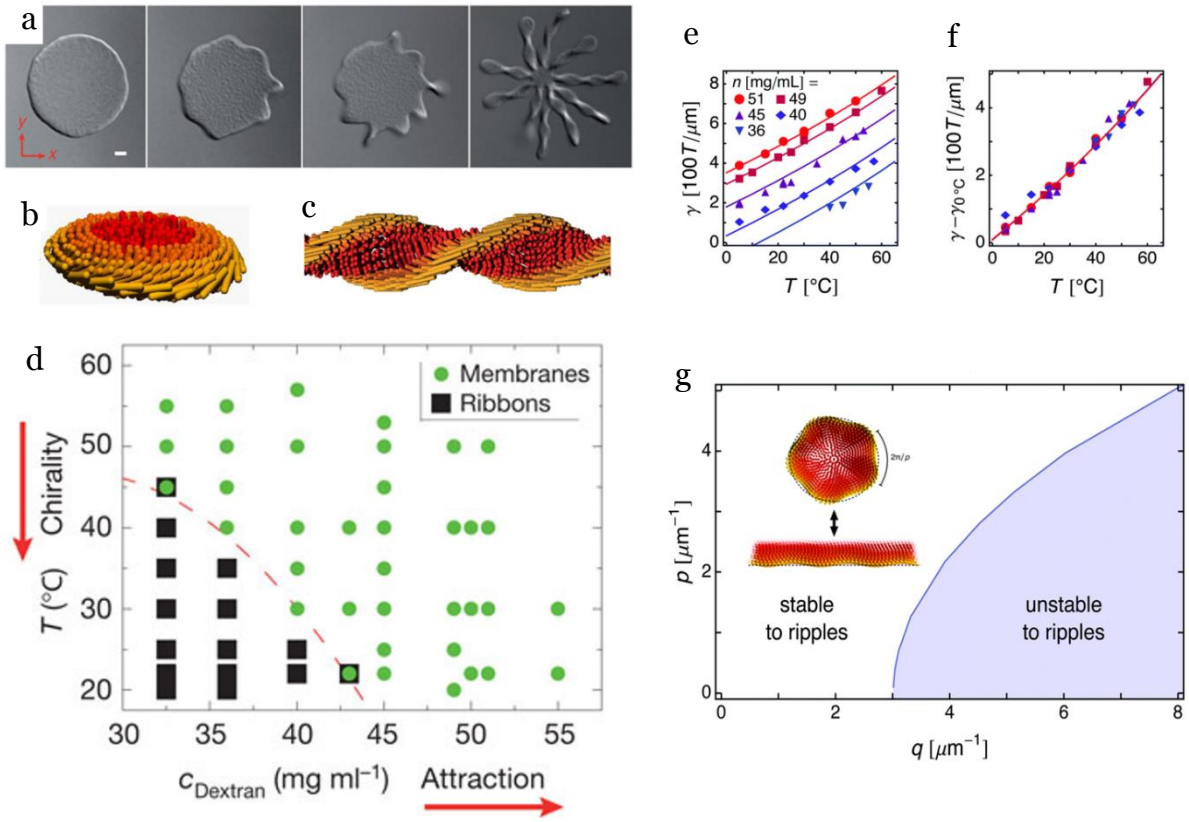

Figure 2. (a) Phase transition from 2D membrane to 1D twisted ribbon by reducing temperature. Scale bar: 2 um. (b-c) Schematic presentation of the monolayer membrane and twisted ribbon. (d) Phase diagram as a function of temperature and Dextran concentration. [95] (e) Linear tension and (f) its relative temperature dependence at various depletant concentration. (g) Unstable ripple wavenumbers p as a function of chiral wavenumber q at

constant Frank-to-depletion ratio 0.85. [98]

3.3 Magnetic field

For rod-shaped particles, the magnetic susceptibility is distinct between the long and short axes. Applied magnetic dipole moments induces an external contribution to the free energy, which causes unbalance in the competition between minimizing self-energy and maximizing configurational entropy, and eventually realign the entire system. [102] One crucial parameter is the anisotropy of magnetic susceptibility $\Delta\chi$. In the case of positive $\Delta\chi$, the particles align their long axis parallel to the magnetic field, and a transition from weakly ordered paranematic phase (field induced temporal alignment from originally isotropic phase) to highly ordered nematic phase occurs by increasing field strength. Both phases are uniaxial in symmetry. For negative $\Delta\chi$, one expects to see rods that are aligned perpendicular to the field, and a uniaxial paranematic shift into a biaxial nematic state with field. [103, 104] In general, most of biological soft materials need very high magnetic field strength for reorientation, because of their limited diamagnetic susceptibility. [80, 91, 105-108] For example, the *fd* virus is significantly realigned when the magnetic field goes above 10 T, then small droplets (tactoids) start to nucleate and grow, and demix into isotropic-nematic coexistence domains. [109] One smart strategy is to decorate the metal nanoparticles with high $|\Delta\chi|$ on the surface of biological filaments. [110, 111] In the amyloid fibrils-Fe_3O_4 nanoparticles hybrid system, as soon as applying a quite weak magnetic field (0.1 T), the disordered phase becomes saturated into an ordered paranematic state. Interestingly, when changing the aspect ratio and volume fraction at a constant dimensionless concentration (**Equation 1**), the stiff fibrils display identical degrees of saturated spatial alignment. On the other hand, semiflexible fibrils with equal dimensionless concentration reach much lower orientation levels due to their semiflexible nature. [59, 104]

3.4 Fluid flow field

The LC orientation under fluid flow is inherently complex, due to its association with hydrodynamics. The fluid flow influences the translational and rotational motion of

constituent rods, and significantly affects the orientational ordering. In turn, the director reorientation shows a kickback effect on fluid motion (termed as backflow). [112] The shear-driven Couette flow has been widely explored, where the emergence of steady-state orientation dynamics, oscillation in a wagging motion, and full tumbling rotation of the director has been theoretically predicted, [113, 114] and experimentally investigated. [115, 116] Another strategy is the directional orientation up on pressure-driven plane Poiseuille flow. [117, 118] Microfluidics provide a platform for precise control of such confined fluid flow in microchannels, where laminar flow is dominant in the usual cases. [119, 120] In general, biological LCs are immediately reoriented along the flow direction with an increased degree of ordering as soon as a very weak flow field is applied. [121] But in the contraction-downstream of microchannel, alignment perpendicular to the microflow direction is detected in the case of amyloid fibrils. [122] Thomas et al. also detected an unexpected perpendicular orientation at the maximum strain rate during the process of DNA compaction in the presence of cationic dendrimers. [123] In general, the mechanical properties of filaments are dependent on the degree of orientational arrangement of rods in nanoscale or molecular levels. [124] Using a flow-field assisted assembly system, well-ordered macro-fibers with exceptionally high strength and stiffness were fabricated by a process that combines microflow induced the alignment and following gelation due to the screening of electrostatic repulsion between cellulose nanofibrils. [125, 126]

3.5 Ice crystal repulsion

The ice crystal has very limited solubility in impurities. [127, 128] Thus, solute in water are favourably accumulated into the non-freezing region during the directional freezing of the aqueous solution, promoting phase separation and a variety of microstructures. [129-131] Indeed, Zhao et al. observed that concentrated and elongated tactoid-like structures spontaneously precipitate after freezing (-20 °C, for > 30 min) and thawing cycling of β-lactoglobulin fibrils suspension, inducing the coexistence of the nematic phase at the bottom and the isotropic phase at the top of the suspension. [60] The concentration range of the

biphasic region is almost 10 times wider than theoretical predictions, although the aspect ratio is reduced to less than 5 folders. However, Corrigan et al. only saw the nematic-to-isotropic phase transition in freeze-thawed hen lysozyme fibrils suspension. [62] That's because the lysozyme fibrils were frozen in liquid nitrogen, and experienced a much lower temperature and faster cooling speed compared with β-lactoglobulin fibrils. Much smaller Ice crystals are generated, [132] and hence milder ice-induced concentrating effect during freezing dynamics, the density of tactoid is not high enough for demixing when thawed. On the other hand, the decrease of aspect ratio due to ice crystal stress drives the transition into disordered state.

3.6 Water evaporation

In the LC solution composed of rod-shaped biopolymers, evaporation process at the air-liquid surface provides potentials to form highly ordered structures. During the drying process of biopolymers having high molecular weight, including DNA, microtubules, and polysaccharides, Kosuke observed the formation of giant microscale micro-domains, which gradually self-integrated and grew into miliscale macro-domain at air-LC interface. [133] By controlling evaporation front of LC solution in a tiny space, they demonstrated that nuclei emerged to grow vertical membrane walls with macroscopic unidirectional orientation. [134, 135] Via evaporation-induced self-assembly process, Uetani indicated that the stiff tunicin nanowhiskers could generate nematic ordering along the perimeter of 2D coffee rings, and form curved discotic 3D microparticles having nematic bundles during spray-drying. But the semiflexible tunicin nanofibers self-organized into flattened microparticles with sharp kinks and rough contours. [136] They further demonstrated that the dry methods and bulk density has limited influence on the pyrolysis behaviour for nanocellulose. [137] Due to the rapid decrease of LC volume under external airflow, Fuller observed an isotropic-cholesteric phase transition of collagen solution on glass substrate. In this desiccation process, collagen fibrils were well oriented, and organized into thin film with cholesteric banding structure in the dried state. [138]

4. Internal force-driven active LC behaviour

The orientational ordering has been experimentally evidenced in a wide range of scales, from nanometer-scale cellular components, connective tissue, to macroscopic fish schools and bird flocks. [24, 26, 139, 140] In this section, we concentrate on the microscopic elongated self-propelled particles, like cytoskeleton assemblies coupled to motor protein, [141-145] motile elongated cells [37, 146-148] and bacteria. [149-151] The rationalization of their organization is crucial for abundant cellular functions (e.g. cell shape maintenance and deformation, migration, growth and division), and might provide significant insights into disclosing the general principle of living systems. [140, 152-154]

4.1 Cytoskeletal assemblies

The building blocks of cytoskeleton in eukaryotic cells, including actin filaments (F-actin), intermediate filaments and microtubules, are quite dynamic and adaptive structures that regulate cellular physical properties and biological functions. [152] Recently, efforts have been focused on the fundamental understanding of the underlying principle for the orientational organization of these protein assemblies, the topological defects, overall cell shape and cellular functions. [155-157] Dogic and his colleagues indicated motile topological defects of active nematics at the water-in-oil interface. [142-144] The non-adsorbing polymer drives microtubules to bundle and accumulate on the water-oil interface; Kinesin clusters bind microtubules and generate an inter-filament sliding force, which further contributes to microtubules extension. The suspended particles are unstable at long wavelength, [158] and topological defects are continuously generated and eliminated at the scale of tens of micrometres, [144] arising from the interaction of the orientational order, topological constraints and activity. A disclination defect of +1/2 has a polarity and generates a flow in a directed fashion, while a -1/2 defect remains stationary under active stress due to the symmetry considerations. [159-162] Moreover, when applying hypertonic stress, the overall vesicle become elliptical and motile, and 4 filopodia-like protrusions are generated from the defect site. [142, 143]

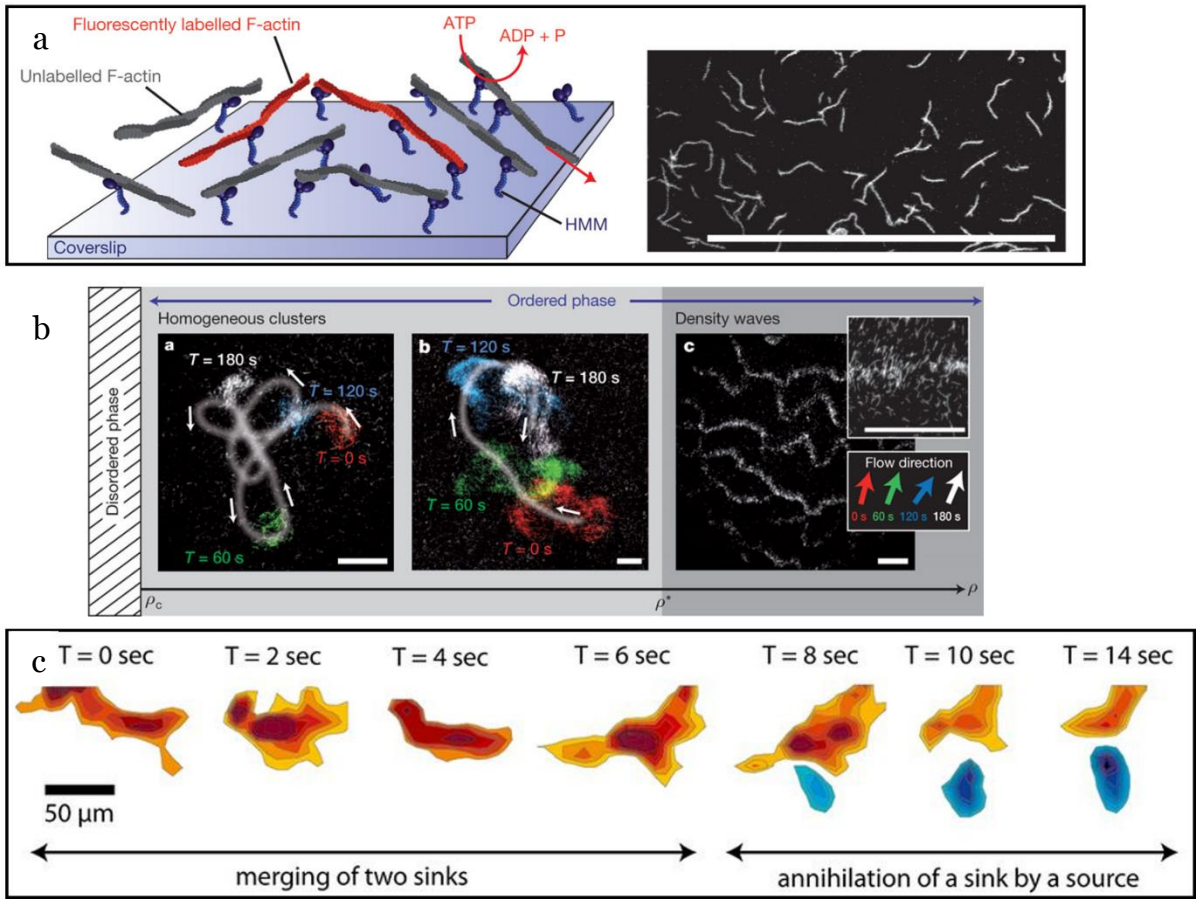

Figure 3. (a) Left: Schematic presentation of motility assay. The motor protein HMM is immobilized on a coverslip, and the fluorescent F-actin is mixed with non-labelled filaments. Right: The individual F-actin moves randomly at low density. (b) The effect of F-actin density on the LC phase behaviours. At intermediate density, the small polar nematic pattern moves independently; bigger but still homogeneous clusters are generated at increased density; in the high-density region spanned wave-like structures moves with high orientational persistence. Scale bar: 50 um. [29, 163] (c) Defect dynamics of ordered cluster. Defects of the same topological charge could merge together, while the ones having opposite charge annihilate each other. [141]

In the actomyosin motility assay, Bausch group demonstrated that when increasing filament density above a critical value, F-actin suspension experienced the disorder-order phase transition, where ordered clusters with a common moving direction coexist with randomly dispersed ones on a 2D glass coverslip substrate, like the isotropic-nematic biphasic

phase in the thermodynamic equilibrium system (**Figure 3**a- b). [29, 141, 163, 164]. Further experimental evidence showed that multi-filament collisions were of central importance for the clumping of particle density during the seeding process, and the transition density was highly dependent on filament length and density. [164, 165] There are always large fluctuations in local particle density coupling to velocity, giving rise to mass flow and destabilization of the large-scale polar. During the continuous moving, defects mostly appear at low particle density, and move from dense to dilute areas. A pair of defects of the same charge could merge and generate a new defect of greater size, while defects with the opposite charge would eliminate each other (**Figure 3**c). [141, 158]

Recent experimental realizations indicate that the organization of the cytoskeleton shows a pronounced association with cellular functions. The enhanced alignment of F-actin in one direction makes cytoskeleton transform from a viscose behaviour to an elastic one and the subsequent shape is elongated remarkably. [166] Small et al. showed that when protrusion occurred in lamellipodia, the F-actin subtended from a wide angular distribution (15–90°) to the front, but once paused they oriented parallel to cell edge, which is crucial for the adaption of slow protrusion and structural support. [167] Schwarz also theoretically demonstrated that the change in filamentous network growth velocity induced a transition between ±35° and +70/0/–70° filament orientation, which is likely related to a force–velocity relationship during cell migration. [168]

4.2 Spindle-shaped cells

A series of studies revealed the formation of well-oriented LC analogues by interacting spindle-shaped cells on a 2D surface. [169] Gruler identified that the migrating and interacting amoeboid cells could transmit surrounding signals, then adapt their own movement and alignment accordingly. When they stick on the substrate for movement, the surface adhesiveness would be modified. Cells would sense the directional variations of substrate adhesiveness and electric file and accumulate to condensed area, then orient their bodies to minimize the environmental signal. [169-172] At the concentration boundary of isotropic-

nematic phase transition, the order parameter is much smaller than that in conventional passive LC. [170] In the ordered domain, there is an anisotropic interaction at small inter-cell distances that drives particles to perfectly align parallel to each other. But layered smectic phase is not formed, probably because the attraction between cells is not strong enough. [172]

In cancerous tumor microenvironments, long-range circumferential alignment of fibroblasts around cancer cells have been often imaged. [173, 174] Theoretical analysis shows that local collision interaction cannot induce the observed ordering in large scale, while the mutual co-alignment between extracellular matrix collagen fibres and fibroblasts plays a critical role in the formation of highly ordered fibroblasts surrounding the tumor cell cluster. [175] Silberzan investigated the dynamics of isolated fibroblast on a flat substrate and realized that the order parameter increased as cells proliferated, but the cell motility was frozen gradually as concentration increased. Due to the cell activity, topological defects pairwise appeared and annihilated when cells processed migration, collision, growth and division on the substrate. They would be trapped in a jammed nematic state as cells got extremely crowded, which would prevent the perfect orientation of the macroscopic biological tissue. [176]

In a densely-packed area, the gliding neural progenitor cells also elongate in shape and align with each another at large scale, like the cell organization in the migratory streams of the adult brain. Due to the cell symmetry, half-integer topological defects are identified in the culture. The density fluctuation, where cells rapidly accumulate at +1/2 charge points and evade -1/2 defects, probably results from the interplay between active force and anisotropic friction. [147, 177] Saw reported on the generation of active nematic behaviour of elongated epithelial tissue during the cellular extrusion process, and demonstrated that compressive stress caused by orientational ordering and topological defect supplied a physical trigger for cell death. [146]

4.3 Motile bacteria

R ecently, the biocompatible LC medium has been used to guide the motion behaviour of dispersed motile bacteria and revealed plentiful dynamic behaviours. [178-182] For

example, Oleg et al. indicated that the self-propelled bacteria Bacillus subtilis can sense the imposed pattern of LC orientation on 2D substrate and move along the LC director (**Figure 4**a-d). They preferably swim toward the positively charged defect and accumulate into an immobilized disk-like colony, while a low density surrounding negatively charges defects. As bacteria activity increases, the uniform ordering of LC starts to destabilize, and experiences formation of bent strip at higher activity; it then nucleates and annihilates into ±1/2 defects and, dynamic turbulence (**Figure 4**d). [178, 180] Mushenheim and colleagues observed that *Proteus mirabilis* were adsorbed to the interface of isotropic tactoid and LC continuous phase. The bacteria moved along the curved interface, and escapes into the surrounding nematic phase at the cusped poles of the tactoid (**Figure 4**e). [183] Since moving bacteria always exert forces to stir the surrounding fluids, the stripe-like domain emerges when concentrated bacteria swims in the LC. [184] The coupling of strong flow localization along the bacteria trajectory and guided bacterial swimming along the LC orientation imply the potential application of cargo transportation (**Figure 4**f-g). [185, 186]

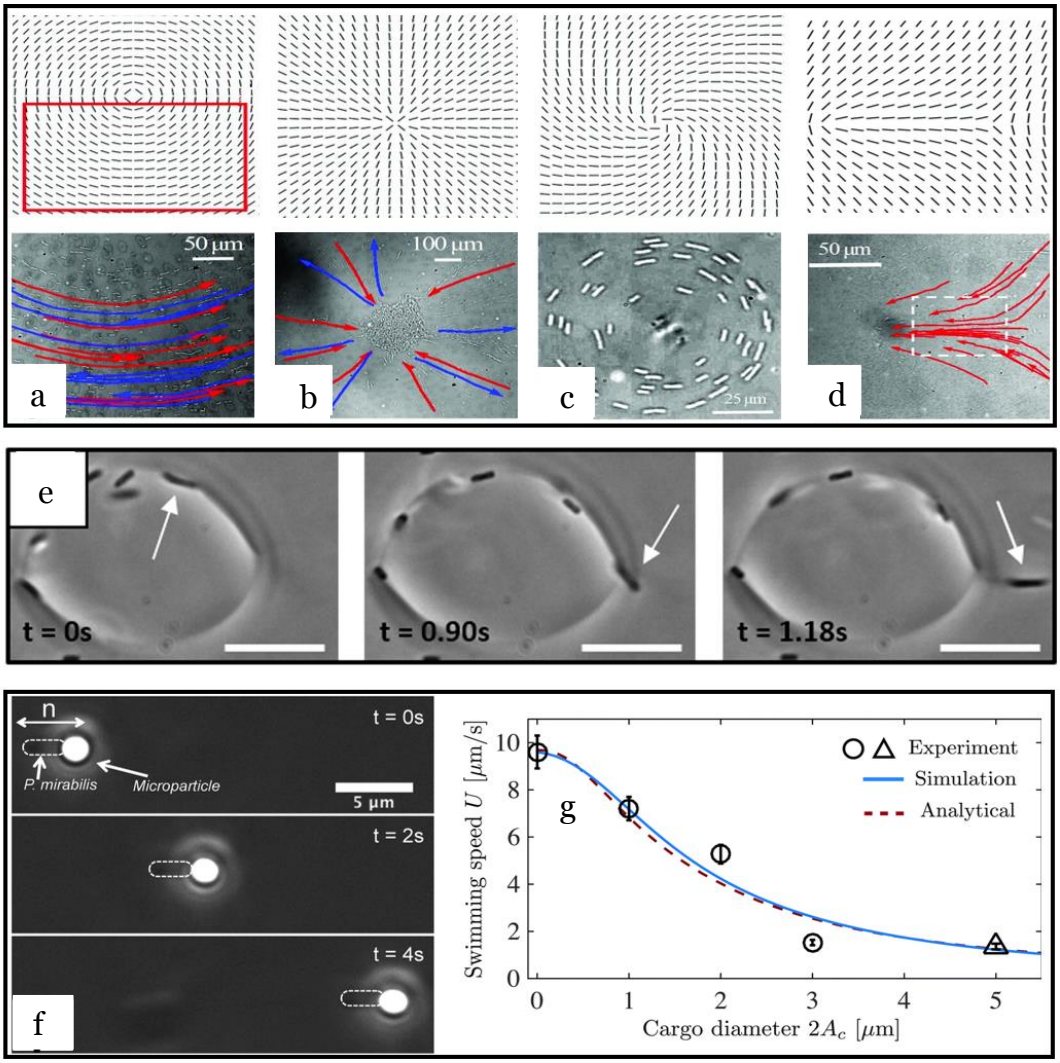

Figure 4. Bipolar motion of bacteria in the pure bend (a) and p splay pattern (b). Unipolar flow around spiralling vortex (c) and motion from -1/2 to +1/2 defects (d). [180] (e) Motion of *P. mirabilis* bacteria along the LC interface, and escape at the cusped pole of the tactoid. [183] (f) *P. mirabilis* cell pushed a polystyrene microparticle along the LC director. (g) Swimming speed of bacteria for cargos having different diameters. [186]

In the pure bacteria system, nematic order could be generated from hydrodynamics, biomechanics and steric interaction. [187-189] The suspension of the motile Bacillus subtilis in an aqueous environment developed a collective zooming bio-nematic (ZBN) phase in a dense domain, and the swimming speed was higher than that of the disordered region. Further

theoretical work suggested that long-range hydrodynamic interaction plays a prime role in the ultimate dynamics of the ZBN state. [150, 189] When concentrated *Bacillus subtilis* suspension was confined in a flattened droplet, Goldstein et al. showed an ordered spiral-vortex flow, where bulk bacteria were oriented to an inward spiralling pattern and pointed outward in the boundary layer. The theoretical analysis indicated that circular confinement and steric interactions control the local bacteria alignment, while hydrodynamic fluid flow generated by swimming bacteria is essential for the large-scale order. [190, 191] When *Escherichia coli* bacteria proliferate on a microfluidic inner channel surface, they push neighbours and generate an expansion flow. Once the population reaches a high enough density, a remarkable transition from a disordered phase to a highly ordered nematic state is formed, where bacteria are aligned along the flow direction. [188]

During the unidirectional motion on an agar surface, the bacteria *Myxococcus xanthus* particles fuse together and aligned well in the same moving direction when colliding with each other. Then, the successive collision and merging of small clusters lead to large moving clusters, and eventually a vortex having multi-layers of rotating discs at high enough density. [30] When lacking nutrition, the bacteria colony transit from a 2D swarm into a 1D stream-like aggregation, where bacteria are aligned along the axis of fruiting body. The bacteria are confined inside it, which significantly decrease the searching areas for nutrient. [192, 193]

5. Summary and outlook

This paper highlights the current understandings of biological LC and addresses the dependence of constituent physical properties on an LC phase diagram, the additional applied stimuli-induced phase transition, and internal force driven active LC behaviours. In the conventional passive LC systems, polydispersity destabilizes a highly ordered phase (e.g. layered smectic phase), as shown in the theoretical prediction by density-functional theory. It would be very interesting to achieve monodispersed rod-shaped assemblies, which may lead to the formation of new LC phases and also be used as a template to fabricate hierarchical structure with higher regularity. Even the stimuli-driven reorientation of biological filaments

has been extensively investigated, realizing the full understanding of subsequent microstructural changes, mechanics and relative applications is still a long-standing challenge.

The theoretical developments for active LC have significantly advanced understanding by extending the relative contexts in addition to traditional soft matter physics. However, there remains much room to progress from the experimental perspective, due to the complexity of biological active matter. One of the potential fields is to explore whether molecular crowding could induce organization of the LC domain, and the possible correlations between a biological structural organization and disease diagnosis. Another field is to achieve programmable reorientation of active LC under external stimuli, we anticipate a wealth of significant work to come even some progresses have emergent in this area. In many cases, the fundamental understanding of spontaneously ordered organization in active matter may offer opportunities of bio-inspired functional materials, for example, motile micro-robotics driven by self-sustained nematic flow, and smart gel with adaptive mechanics upon applied fields.

Acknowledgements
This work was financially supported by the National Natural Science Foundation of China (21374089), the Natural Science Basic Research Plan in Shaanxi Province of China (2018JC-008, Distinguished Young Scholar) and the Engineering and Physical Sciences Research Council (EPSRC) grants-EP/N007921/1 and EP/N032861/1.

Conflict of Interest
The authors declare no conflict of interest.

References

[1] A. D. Rey, *Soft Matter* **2010,** *6*, 3402-3429.

[2] M. Mitov, *Soft Matter*, **2017**, 13, 4176-4209.

[3] I. W. Hamley, *Soft Matter*, **2010**, 6, 1863-1871.

[4] Q. Li, Liquid Crystals Beyond Displays: Chemistry, Physics, and Applications, Wiley: New Jersey, **2012**.

[5] L. Onsager, *Annals of the New York Academy of Sciences* **1949,** *51*, 627-659.

[6] J. Zhao, *Doctoral thesis,* ETH Zurich, July, **2016**.

[7] Y. Li, H. Miao, H. R. Ma, J. Z. Y. Chen, *RSC Adv* **2014,** *4*, 27471-27480.

[8] Y. Li, H. Miao, H. R. Ma, J. Z. Y. Chen, *Soft Matter* **2013,** *9*, 11461-11466.

[9] R. Zhang, Y. Zhou, J. A. Martinez-Gonzalez, J.P. Hernandez-Ortiz, N. L. Abbott, J. J. de Pablo, *Sci Adv* **2016,** *2*. e1600978.

[10] S. J. Woltman, G. D. Jay, G. P. Crawford, *Liquid Crystals: Frontiers in Biomedical Applications*. World Scientific: New Jersey, **2007**.

[11] S. J. Woltman, G. D. Jay, G. P. Crawford, *Nat Mater*, **2007**, 6, 929-938.

[12] L. Wang, H. Dong, Y. N. Li, C. M. Xue, L. D. Sun, C. H. Yan, Q. Li, *J Am Chem Soc*, **2014**, 136, 4480-4483.

[13] A. Angelova, B. Angelov, R. Mutafchieva, S. Lesieur, P. Couvreur, *Accounts Chem Res*, **2011**, 44, 147-156.

[14] D. Wang, L. Zhu, J. F. Chen, L. M. Dai, *Angew Chem Int Ed Engl*, **2016**, 55, 10795-10799.

[15] E. Bukusoglu, M. B. Pantoja, P. C. Mushenheim, X. G. Wang, N. L. Abbott, *Annu Rev Chem Biomol* **2016,** *7*, 163-196.

[16] P. van der Asdonk, P. H. J. Kouwer, *Chem Soc Rev* **2017,** *46*, 5935-5949.

[17] L. Wang, A. M. Urbas, Q. Li, *Adv Mater* **2018**, 30, 1801335.

[18] L. Wang, H. K. Bisoyi, Z. G. Zheng, K. G. Gutierrez-Cuevas, G. Singh, S. Kumar, T. J. Bunning, Q. Li, *Mater Today*, **2017**, 20, 230-237.

[19] Z. G. Zheng, Y. N. Li, H. K. Bisoyi, L. Wang, T. J. Bunning, Q. Li, *Nature*, **2016**, 532, 352-356.

[20] L. Wang, Q. Li, *Chem Soc Rev*, **2018**, 47, 1044-1097.

[21] L. Wang, *Liq Cryst*, **2016**, 43, 2062-2078.

[22] L. Wang, H. Dong, Y. N. Li, R. Liu, Y. F. Wang, H. K. Bisoyi, L. D. Sun, C. H. Yan, Q. Li, *Advanced Materials*, **2015**, 27, 2065-2069.

[23] L. Wang, D. Chen, K. G. Gutierrez-Cuevas, H. K. Bisoyi, J. Fan, R. S. Zola, G. Li, A. M. Urbas, T. J. Bunning, D. A. Weitz, Q. Li, *Mater Horiz*, **2017**, 4, 1190-1195.

[24] S. Ramaswamy, *Annu Rev Condens Matter P,* **2010,** *1*, 323-345.

[25] A. Doostmohammadi, J. Ignes-Mullol, J. M. Yeomans, F. Sagues, *Nat Commun* **2018,** *9*, 3246.

[26] M. C. Marchetti, J. F. Joanny, S. Ramaswamy, T. B. Liverpool, J. Prost, M. Rao, R. A. Simha, *Rev Mod Phys* **2013,** *85*, 1143.

[27] S. Ramaswamy, *J Stat Mech*, **2017**, 054002.

[28] A. Doostmohammadi, T. B. Saw, V. Nier, L. Kocgozlu, S. P. Thampi, Y. Toyama, P. Marcq, C. T. Lim, J. M. Yeomans, B. Ladoux, *Eur Biophys J Biophy* **2017,** *46*, S243-S243.

[29] V. Schaller, C.Weber, C. Semmrich, E. Frey, A. R.Bausch, *Nature* **2010,** *467*, 73-77.

[30] J. Starruss, F. Peruani, V. Jakovljevic, L. Sogaard-Andersen, A.Deutsch, M. Bar, *Interface Focus* **2012,** *2*, 774-785.

[31] A. M. Menzel, *Phys Rep* **2015,** *554*, 1-45.

[32] Y. Sumino, K. H. Nagai, Y. Shitaka, D. Tanaka, K. Yoshikawa, H. Chate,; K. Oiwa, *Nature* **2012,** *483*, 448-452.

[33] G. Duclos, C. Blanch-Mercader, V. Yashunsky, G. Salbreux, J. F. Joanny, J. Prost, P. Silberzan, *Nat Phys* **2018,** *14*, 728-732.

[34] T. Gao, Z. R. Li, *Phys Rev Lett* **2017,** *119*, 108002.

[35] L. Giomi, A. DeSimone, *Phys Rev Lett* **2014,** *112*, 147802.

[36] C. Blanch-Mercader, V. Yashunsky, S. Garcia, G. Duclos, L. Giomi, P. Silberzan, *Phys Rev Lett* **2018,** *120*, 208101.

[37] G. Duclos, C. Erlenkamper, J. F. Joanny, P. Silberzan, *Nat Phys* **2017,** *13*, 58-62.

[38] R. L. Rill, T. E. Strzelecka, M. W. Davidson, D. H. Vanwinkle, *Physica a-Stat Mech Appl* **1991,** *176*, 87-116.

[39] J. Pelta, D. Durand, J. Doucet, F.Livolant, *Biophys J* **1996,** *71*, 48-63.

[40] F. Livolant, A. Leforestier, *Prog Polym Sci* **1996,** *21*, 1115-1164.

[41] T. E. Strzelecka, M. W. Davidson, R. L. Rill, *Nature* **1988,** *331*, 457-460.

[42] M. Siavashpouri, C. H. Wachauf, M. J. Zakhary, F. Praetorius, H. Dietz,; Z. Dogic, *Nat Mater* **2017,** *16*, 849-856.

[43] T. Bellini, G. Zanchetta, T. P. Fraccia, R. Cerbino, E. Tsai, G. P. Smith, M. J. Moran, D. M. Walba, N. A. Clark, *Proc Natl Acad Sci USA* **2012,** *109*, 1110-1115.

[44] K. Osada, H. Oshima, D. Kobayashi, M. Doi, M. Enoki, Y. Yamasaki, K. Kataoka, *J Am Chem Soc*, **2010**, 132, 12343-12348.

[45] K. Osada, T. Shiotani, T. A. Tockary, D. Kobayashi, H. Oshima, S. Ikeda, R. J. Christie, K. Itaka, and K. Kataoka, *Biomaterials*, **2012**, 33, 325-332.

[46] M. M. Giraud-Guille, G. Mosser, E. Belamie, *Curr Opin Colloid Interface Sci* **2008,** *13*, 303-313.

[47] C. R. Safinya, J. Deek, R. Beck, J. B. Jones, Y. L. Li, *Annu Rev Conden Ma P* **2015,** *6*, 113-136.

[48] D. G. Gray, *Philos T R Soc A* **2018,** *376*, 2112.
[49] Y. Habibi, L. A. Lucia, O. J. Rojas, Chem Rev, **2010**, 110, 3479-3500.
[50] A. Isogai, T. Saito, H. Fukuzumi, *Nanoscale*, **2011**, 3, 71-85.
[51] K. Uetani, T. Okada, H. T. Oyama, *Biomacromolecules*, **2015**, 16, 2220-2227.
[52] J. X. Tang, S. Fraden, *Liq Cryst* **1995,** *19*, 459-467.
[53] K. R. Purdy, S. Varga, A. Galindo, G. Jackson, S. Fraden, *Phys Rev Lett* **2005,** *94*, 057801.
[54] J. X. Tang, S. Fraden, *Biopolymers* **1996,** *39*, 13-22.
[55] S. Fraden, G. Maret, D. L. D. Caspar, R. B. Meyer, *Phys Rev Lett* **1989,** *63*, 2068-2071.
[56] J. M. Jung, R. Mezzenga, *Langmuir* **2010,** *26*, 504-514.
[57] R. Mezzenga, J. M. Jung, J. Adamcik, *Langmuir* **2010,** *26*, 10401-10405.
[58] J. G. Zhao,; C. X. Li,; R. Mezzenga, *J Phys-Condens Mat* **2014,** *26*,464112.
[59] J. Zhao, S. Bolisetty, S. Isabettini, J. Kohlbrecher, J. Adamcik, P. Fischer, R. Mezzenga, *Biomacromolecules* **2016,** *17*, 2555-2561.
[60] J. G. Zhao, S. Bolisetty, J. Adamcik, J. Han, M. P. Fernandez-Ronco, R. Mezzenga, *Langmuir* **2016,** *32*, 2492-2499.
[61] D. Vigolo, J. G. Zhao, S. Handschin, X. B. Cao, A. J. Demello, R. Mezzenga, *Sci Rep* **2017,** *7*, 1211.
[62] A. M. Corrigan, C. Muller, M. R. H. Krebs, *J Am Chem Soc* **2006,** *128*, 14740-14741.
[63] C. Muller, O. Inganas, *J Mater Sci* **2011,** *46*, 3687-3692.
[64] D. Cannon, A. M. Donald, *Soft Matter* **2013,** *9*, 2852-2857.
[65] A. Poniewierski, T. J. Sluckin, *Phys Rev A* **1991,** *43*, 6837-6842.
[66] P. Bolhuis, D. Frenkel, *J Chem Phys* **1997,** *106*, 666-687.
[67] J. Viamontes, P. W. Oakes, J. X. Tang, *Phys Rev Lett* **2006,** *97*,118103.
[68] H. N. W. Lekkerkerker, P. Coulon, R. Vanderhaegen, R. Deblieck, *J Chem Phys* **1984,** *80*, 3427-3433.
[69] H. H. Wensink, G. J. Vroege, *J Chem Phys* **2003,** *119*, 6868-6882.
[70] G. J. Vroege, H. N. W. Lekkerkerker, *J Phys Chem* **1993,** *97*, 3601-3605.
[71] A. Speranza, P. Sollich, *J Chem Phys* **2002,** *117*, 5421-5436.
[72] T. M. Birshtein, B. I. Kolegov, V. A. Pryamitsyn, *Polym Sci(U.S.S.R.)* **1988,** *30*, 316-324.
[73] P. C. Hiemenz, T. P. Lodge, *Polymer chemistry*. CRC Press: Boca Raton, **2007**.
[74] C. P. Broedersz, F. C. MacKintosh, *Rev Mod Phys* **2014,** *86*, 995-1036.
[75] K. R. Purdy, S. Fraden, *Phys Rev E* **2004,** *70*, 061703.
[76] A. R. Khokhlov, A. N. Semenov, *Physica A* **1981,** *108*, 546-556.
[77] A. R. Khokhlov, A. N. Semenov, *Physica A* **1982,** *112*, 605-614.

[78] Z. Y. Chen, *Macromolecules* **1993,** *26*, 3419-3423.
[79] X. M. Dong, T. Kimura, J. F. Revol, D. G. Gray, *Langmuir* **1996,** *12*, 2076-2082.
[80] E. Belamie, P. Davidson, M. M. Giraud-Guille, *J Phys Chem B* **2004,** *108*, 14991-15000.
[81] X. M. Dong, D. G. Gray, *Langmuir* **1997,** *13*, 2404-2409.
[82] A. Stroobants, H. N. W. Lekkerkerker, T. Odijk, *Macromolecules* **1986,** *19*, 2232-2238.
[83] L. Wang and Q. Li, *Adv Funct Mater*, **2016**, 26, 10-28.
[84] Z. Dogic, K. R. Purdy, E. Grelet, M. Adams, S. Fraden, *Phys Rev E* **2004,** *69*, 051702.
[85] M. Adams, S. Fraden, *Biophys J* **1998,** *74*, 669-677.
[86] C. D. Edgar, D. G. Gray, *Macromolecules* **2002,** *35*, 7400-7406.
[87] S. Asakura, F. Oosawa, *J Chem Phys* **1954,** *22*, 1255-1256.
[88] S. Asakura,; F. Oosawa, *J Polym Sci* **1958,** *33*, 183-192.
[89] J. F. Joanny, L. Leibler, P. G. Degennes, *J Polym Sci Pol Phys* **1979,** *17*, 1073-1084.
[90] G. J. Thomas, L. A. Day, *Proc Natl Acad Sci USA* **1981,** *78*, 2962-2966.
[91] J. Torbet, G. Maret, *Biopolymers* **1981,** *20*, 2657-2669.
[92] G. Maret, M. V. Schickfus, A. Mayer, K. Dransfeld, *Phys Rev Lett* **1975,** *35*, 397-400.
[93] L. A. Day, C. J. Marzec, S. A. Reisberg, A. Casadevall, *Annu Rev Biophys Bio*, **1988**, 17, 509-539.
[94] F. Tombolato, A. Ferrarini, E. Grelet, *Phys Rev Lett*, **2006**, 96, 258302.
[95] T. Gibaud, E. Barry, M. J. Zakhary, M. Henglin, A. Ward,; Y. S. Yang, C. Berciu, R. Oldenbourg, M. F. Hagan, D. Nicastro, R. B. Meyer, Z. Dogic, *Nature* **2012,** *481*, 348-351.
[96] M. J. Zakhary, T. Gibaud, C. N. Kaplan, E. Barry, R. Oldenbourg, R. B. Meyer, Z. Dogic, *Nat Commun* **2014,** *5*, 3063.
[97] L. L. Jia, M. J. Zakhary, Z. Dogic, R. A. Pelcovits, T. R. Powers, *Phys Rev E*, **2017**, 95, 060701.
[98] L. Kang, T. Gibaud, Z. Dogic, T. C. Lubensky, *Soft Matter*, **2016**, 12, 386-401.
[99] R. Piazza, A. Parola, *J Phys-Condens Mat* **2008,** *20*,153102.
[100] S. Iacopini, R. Piazza, *Europhys Lett* **2003,** *63*, 247-253.
[101] S. Iacopini, R. Rusconi, R. Piazza, *Eur Phys J E* **2006,** *19*, 59-67.
[102] H. H. Wensink, G. J. Vroege, *Phys Rev E* **2005,** *72*, 031708.
[103] B. J. Lemaire, P. Davidson, J. Ferre, J. P. Jamet, D. Petermann, P. Panine, I. Dozov, D. Stoenescu, J. P. Jolivet, *Faraday Discuss* **2005,** *128*, 271-283.
[104] A. R. Khokhlov, A. N. Semenov, *Macromolecules* **1982,** *15*, 1272-1277.
[105] J. Torbet, G. Maret, *J Mol Biol* **1979,** *134*, 843-845.
[106] E. Senechal, G. Maret, K. Dransfeld, *Int J Biol Macromol* **1980,** *2*, 256-262.
[107] G. Maret, K. Dransfeld, *Top Appl Phys* **1985,** *57*, 143-204.

[108] R. J. A. Hill, V. L. Sedman, S. Allen, P. M. Williams, M. Paoli, L. Adler-Abramovich, E. Gazit, L. Eaves, S. J. B. Tendler, *Adv Mater* **2007,** *19*, 4474-4479.
[109] J. X. Tang, S. Fraden, *Phys Rev Lett* **1993,** *71*, 3509-3512.
[110] F. Brochard, P. G. D. Gennes, *J Phys-Paris* **1970,** *31*, 691-708.
[111] S. H. Chen, N. M. Amer, *Phys Rev Lett* **1983,** *51*, 2298-2301.
[112] F. Brochard, *Mol Cryst Liq Cryst* **1973,** *23*, 51-58.
[113] G. Rienacker, S. Hess, *Physica A* **1999,** *267*, 294-321.
[114] M. Doi, *J Polym Sci Pol Phys* **1981,** *19*, 229-243.
[115] T. A. J. Lenstra, Z. Dogic, J. K. G. Dhont, *J Chem Phys* **2001,** *114*, 10151-10162.
[116] M. P. Lettinga, Z. Dogic, H. Wang, J. Vermant, *Langmuir* **2005,** *21*, 8048-8057.
[117] H. See, M. Doi, R. Larson, *J Chem Phys* **1990,** *92*, 792-800.
[118] J. Feng, L. G. Leal, *Phys Fluids* **1999,** *11*, 2821-2835.
[119] H. A. Stone, A. D. Stroock, A. Ajdari, *Annu Rev Fluid Mech* **2004,** *36*, 381-411.
[120] T. M. Squires, S. R. Quake, *Rev Mod Phys* **2005,** *77*, 977-1026.
[121] B. F. B. Silva, *Phys Chem Chem Phys* **2017,** *19*, 23690-23703.
[122] V. Lutz-Bueno, J. G. Zhao, R. Mezzenga, T. Pfohl, P. Fischer, M. Liebi, *Lab Chip* **2016,** *16*, 4028-4035.
[123] T. Pfohl, A. Otten, S. Koster, R. Dootz, B. Struth, H. M. Evans, *Biomacromolecules* **2007,** *8*, 2167-2172.
[124] F. Barthelat, Z. Yin, M. J. Buehler, *Nat Rev Mater* **2016,** *1*, 16007.
[125] K. M. O. Hakansson, A. B. Fall, F. Lundell, S. Yu, C. Krywka, S. V. Roth, G. Santoro, M. Kvick, L. P. Wittberg, L. Wagberg, L. D. Soderberg, *Nat Commun* **2014,** *5*, 5018.
[126] N. Mittal, F. Ansari, V. K. Gowda, C. Brouzet, P. Chen, P. T. Larsson, S. V. Roth, F. Lundell, L. Wagberg, N. A. Kotov, L. D.Soderberg, *ACS Nano* **2018,** *12*, 6378-6388.
[127] R. Halde, *Water Res* **1980,** *14*, 575-580.
[128] M. Spannuth, S. G. J. Mochrie, S. S. L. Peppin, J. S. Wettlaufer, *J Chem Phys* **2011,** *135*, 224706.
[129] J. P. Dong, A. Hubel, J. C. Bischof, A. Aksan, *J Phys Chem B* **2009,** *113*, 10081-10087.
[130] A. Twomey, R. Less, K. Kurata, H. Takamatsu, A. Aksan, *J Phys Chem B* **2013,** *117*, 7889-7897.
[131] S.Scanlon, A. Aggeli, N. Boden, T. C. B. McLeish, P. Hine, R. J. Koopmans, C. Crowder, *Soft Matter* **2009,** *5*, 1237-1246.
[132] S. Deville, E. Saiz, A. P. Tomsia, *Acta Mater* **2007,** *55*, 1965-1974.
[133] K. Okeyoshi, M. K. Okajima, T. Kaneko, *Biomacromolecules*, **2016**, 17, 2096-2103.
[134] K. Okeyoshi, M. K. Okajima, T. Kaneko, *Sci Rep-UK*, **2017**, 7, 5615.

[135] K. Okeyoshi, G. Joshi, M. K. Okajima, T. Kaneko, *Adv Mater Interfaces*, **2018**, 5, 1701219.
[136] K. Uetani, H. Yano, *Soft Matter*, **2013**, 9, 3396-3401.
[137] K. Uetani, Y. Watanabe, K. Abe, H. Yano, *Cellulose*, **2014**, 21, 1631-1643.
[138] J. E. Kirkwood and G. G. Fuller, *Langmuir*, **2009**, 25, 3200-3206.
[139] A. Ciferri, *Chem Rev* **2016,** *116*, 1353-1374.
[140] T. J. Wess, *Adv Protein Chem* **2005,** *70*, 341-374.
[141] V. Schaller, A. R. Bausch, *Proc Natl Acad Sci USA* **2013,** *110*, 4488-4493.
[142] T. Sanchez, D. T. N. Chen, S. J. DeCamp, M. Heymann, Z. Dogic, *Nature* **2012,** *491*, 431-434.
[143] F. C. Keber, E. Loiseau, T. Sanchez, S. J. DeCamp, L. Giomi, M. J. Bowick, M. C. Marchetti, Z. Dogic, A. R. Bausch, *Science* **2014,** *345*, 1135-1139.
[144] S. J. DeCamp, G. S. Redner, A. Baskaran, M. F. Hagan, Z. Dogic, *Nat Mater* **2015,** *14*, 1110-1115.
[145] P. Guillamat, J. Ignes-Mullol, F. Sagues, *Proc Natl Acad Sci USA* **2016,** *113*, 5498-5502.
[146] T. B. Saw, A. Doostmohammadi, V. Nier, L. Kocgozlu, S. Thampi, Y. Toyama, P. Marcq, C. T. Lim, J. M. Yeomans, B. Ladoux, *Nature* **2017,** *544*, 212-216.
[147] K. Kawaguchi, R. Kageyama, M. Sano, *Nature* **2017,** *545*, 327-332.
[148] G. Duclos, S. Garcia, H. G. Yevick, P. Silberzan, *Soft Matter* **2014,** *10*, 2346-2353.
[149] H. H. Wensink, J. Dunkel, S. Heidenreich, K. Drescher, R. E. Goldstein, H. Lowen, J. M. Yeomans, *Proc Natl Acad Sci USA* **2012,** *109*, 14308-14313.
[150] L. H. Cisneros, R. Cortez, C. Dombrowski, R. E. Goldstein, J. O. Kessler, *Exp Fluids* **2007,** *43*, 737-753.
[151] R. Hartmann, P. K. Singh, P. Pearce, R. Mok, B. Song, F. Díaz-Pascual, J. Dunkel, K. Drescher, *Nat Phys* **2018**, DOI 10.1038/s41567-018-0356-9.
[152] D. A. Fletcher, D. Mullins, *Nature* **2010,** *463*, 485-492.
[153] G. Popkin, *Nature* **2016,** *529*, 16-18.
[154] M. Leoni, O. V. Manyuhina, M. J. Bowick, M. C. Marchetti, *Soft Matter* **2017,** *13*, 1257-1266.
[155] R. Zhang, Y. Zhou, M. Rahimi, J. J. de Pablo, *Nat Commun* **2016,** *7*, 13483.
[156] R. Zhang, N. Kumar, J. L. Ross, M. L. Gardel, J. J. de Pablo, *Proc Natl Acad Sci USA* **2018,** *115*, E124-E133.
[157] P. W. Ellis, D. J. G. Pearce, Y. W. Chang, G. Goldsztein, L. Giomi, A. Fernandez-Nieves, *Nat Phys* **2018,** *14*, 85-90.
[158] R. A. Simha, S. Ramaswamy, *Phys Rev Lett* **2002,** *89*, 058101.
[159] L. Giomi, M. J. Bowick, X. Ma, M. C. Marchetti, *Phys Rev Lett* **2013,** *111*, 209901.

[160] S. P. Thampi, R. Golestanian, J. M. Yeomans, *Phys Rev Lett* **2013,** *111*, 118101.
[161] X. Q. Shi, Y. Q. Ma, *Nat Commun* **2013,** *4*, 3013.
[162] L. Giomi, M. J. Bowick, X. Ma, M. C. Marchetti, *Phys Rev Lett* **2013,** *110*, 228101.
[163] V. Schaller, C. Weber, E. Frey, A. R. Bausch, *Soft Matter* **2011,** *7*, 3213-3218.
[164] R. Suzuki, A. R. Bausch, *Nat Commun* **2017,** *8*, 41.
[165] R. Suzuki, C. A. Weber, E. Frey, A. R. Bausch, *Nat Phys* **2015,** *11*, 839-843.
[166] M. Gupta, B. R. Sarangi, J. Deschamps, Y. Nematbakhsh, A. Callan-Jones, F. Margadant, R. M. Mege, C. T. Lim, R. Voituriez, B. Ladoux, *Nat Commun* **2015,** *6*, 8525.
[167] S. A. Koestler, S. Auinger, M. Vinzenz, K. Rottner, J. V. Small, *Nat Cell Biol* **2008,** *10*, 306-313.
[168] J. Weichsel, U. S. Schwarz, *Proc Natl Acad Sci USA* **2010,** *107*, 6304-6309.
[169] H. Gruler, *Liq Cryst* **1998,** *24*, 49-66.
[170] H. Gruler, U. Dewald, M. Eberhardt, *Eur Phys J B* **1999,** *11*, 187-192.
[171] R. Kemkemer, D. Kling, D. Kaufmann, H. Gruler, *Eur Phys J E* **2000,** *1*, 215-225.
[172] R. Kemkemer, V. Teichgraber, S. Schrank-Kaufmann, D. Kaufmann, H. Gruler, *Eur Phys J E* **2000,** *3*, 101-110.
[173] J. Tommelein, L. Verset, T. Boterberg, P. Demetter, M. Bracke, O. De Wever, *Front Oncol* **2015,** *5*, 63.
[174] B. C. Ozdemir, T. Pentcheva-Hoang, J. L. Carstens, X. Zheng, C. C. Wu, T. R. Simpson, H. Laklai, H. Sugimoto, C. Kahlert, S. V. Novitskiy, A. De Jesus-Acosta, P. Sharma, P. Heidari, U. Mahmood, L. Chin, H. L. Moses, V. M. Weaver, A. Maitra, J. P. Allison, V. S. LeBleu, R. Kalluri, *Cancer Cell* **2015,** *28*, 831-833.
[175] X. Li, R. Balagam, T. F. He, P. P. Lee, O. A. Igoshin, H. Levine, *Proc Natl Acad Sci USA* **2017,** *114*, 8974-8979.
[176] G. Duclos, S. Garcia, H. G. Yevick, P. Silberzan, *Soft Matter* **2014,** *10*, 2346-2353.
[177] C. Lois, J. M. Garcia-Verdugo, A. Alvarez-Buyll, *Science* **1996,** *271*, 978-81.
[178] S. Zhou, A. Sokolov, O. D. Lavrentovich, I. S. Aranson, *Proc Natl Acad Sci USA* **2014,** *111*, 1265-1270.
[179] P. C. Mushenheim, R. R. Trivedi, S. S. Roy, M. S. Arnold, D. B. Weibel, N. L. Abbott, *Soft Matter* **2015,** *11*, 6821-6831.
[180] C. H. Peng, T. Turiv, Y. B. Guo, Q. H. Wei, O. D. Lavrentovich, *Science* **2016,** *354*, 882-885.
[181] M. M. Genkin, A. Sokolov, O. D. Lavrentovich, I. S. Aranson, *Phys Rev X* **2017,** *7*, 011029.
[182] S. Zhou, *Lyotropic Chromonic Liquid Crystals*, Springer: Cham, **2017**.
[183] P. C. Mushenheim, R. R. Trivedi, D. B. Weibel, N. L. Abbott, *Biophys J*, **2014**, 107, 255–65.

[184] P. C. Mushenheim, R. R. Trivedi, H. H. Tuson, D. B. Weibel, N. L. Abbott, *Soft Matter* **2014,** *10*, 88-95.
[185] A. Sokolov, S. Zhou, O. D. Lavrentovich, I. S. Aranson, *Phys Rev E* **2015,** *91*, 013009.
[186] R. R. Trivedi, R. Maeda, N. L. Abbott, S. E. Spagnolie, D. B. Weibel, *Soft Matter* **2015,** *11*, 8404-8408.
[187] H. P. Zhang, A. Be'er, E. L. Florin, H. L. Swinney, *Proc Natl Acad Sci USA* **2010,** *107*, 13626-13630.
[188] D. Volfson, S. Cookson, J. Hasty, L. S. Tsimring, *Proc Natl Acad Sci USA* **2008,** *105*, 15346-15351.
[189] L. H. Cisneros, J. O. Kessler, S. Ganguly, R. E.Goldstein, *Phys Rev E* **2011,** *83*, 061907.
[190] H. Wioland, F. G. Woodhouse, J. Dunkel, J. O. Kessler, R. E. Goldstein, *Phys Rev Lett* **2013,** *110*, 268102.
[191] E. Lushi, H. Wioland, R. E. Goldstein, *Proc Natl Acad Sci USA* **2014,** *111*, 9733-9738.
[192] S. Thutupalli, M. Z. Sun, F. Bunyak, K. Palaniappan, J. W. Shaevitz, *J R Soc Interface* **2015,** *12*, 20150049.
[193] D. R. Zusman, A. E. Scott, Z. Yang, J. R. Kirby, *Nat Rev Microbiol* **2007,** *5*, 862-872.
[194] A. M. Bohle, R. Holyst, T. Vilgis, *Phys Rev Lett* **1996,** *76*, 1396-1399.

The Table of Contents Entry

Advances in Biological Liquid Crystals

Dr. Jianguo Zhao, Dr. Utku Gulan, Dr. Takafumi Horie, Prof. Naoto Ohmura, Dr. Jun Han, Prof. Chao Yang, Prof. Jie Kong, Dr. Steven Wang*, Dr. Ben Bin Xu**

ToC figure